Journal of the Korean Nuclear Society
Volume 29, Number 1, pp. 15~24, February 1997

Design and Evaluation of the Model Based Controller for a U-tube Steam Generator Level

Keung Koo Kim, Doojeong Lee
Korea Atomic Energy Research Institute
150 Dukjin-dong, Yusong-gu, Taejon 305-353, Korea

John E. Meyer, David D. Lanning
Department of Nuclear Engineering
Massachusetts Institute of Technology 77 Massachusetts Ave, Cambridge, MA02139

John A. Bernard
MIT Nuclear Reactor Laboratory
138 Albany St., Cambridge, MA02139

(Received March 21, 1996)

Abstract

The design and evaluation of a digital U-tube steam generator level controller of nuclear power plants, which uses model-based compensators to offset the inverse response behavior of water level, is described. Included is a review of steam generator level dynamics, a simulation model that replicates the effects of feedwater and steam flowrate as well as temperature on steam generator level, the design of both the compensators and the overall controller, and the results of simulation studies in which the performances of this model-based controller and existing analog ones were compared. The proposed digital steam generator level controller is stable and its use significantly improves the controllability of steam generator level.

1. Introduction

This paper reports the design and evaluation via simulation of a compensator-based method for the digital control of level on steam generators. These devices, which are typically sixty-eight feet high and fourteen feet in diameter, contain thousands of U-shaped tubes that are used to transfer heat from the primary to the secondary side of nuclear pressurized water reactors (PWRs). Specifically, the energy that is generated from fission in a PWR is transferred from the reactor core to the primary coolant which is typically at a temperature and pressure of 540 °F and 2250 psi. When this coolant flows through the steam generator's tube bundle, heat is transferred to the secondary coolant which, being at about 1000 psi pressure, boils to form the steam that drive the turbines. The proper control of water level on the secondary side of a steam generator is essential because too low a level may portend insufficient energy removal from the reactor while too high a level will degrade steam quality and in turn cause erosion of the tur-

bine blades. Unfortunately, steam generator level control is complicated by counterintuitive dynamics in which an inverse response effect known as 'shrink and swell' causes the water level to respond initially in a manner opposite to its long-term asymptotic behavior. This phenomenon has been identified as a major contributor to unanticipated plant shutdowns [1].

Existing analog steam generator level controllers use both level and flow measurements to generate the appropriate control signal. The former provides feedback based on the actual level error while the latter is a feedforward action that anticipates a level error. Unfortunately, the flow measurements are too uncertain for reliable use during low power operation and as a result current analog level controllers may not provide satisfactory performance at low power. Therefore, two different control logics for low and high power level, may be used and sometimes the level is controlled manually. Manual control may also be unsatisfactory because even skilled operators may have difficulty in reacting properly to an inverse response. In particular, operators sometimes overcompensate when restoring level and, in so doing, cause a reactor trip. The purpose of the research reported here was to develop a superior means of control through the application of a digital compensator.

The specific objectives of this paper are to : (1) review steam generator water level dynamics, (2) design a simplified model of a steam generator, (3) discuss the design of the water level controller with emphasis on the model-based compensators, and (4) present the results of simulation studies that demonstrate the performance of the proposed controller.

2. Steam Generator Dynamic

Figure 1 is a schematic diagram of a U-tube steam generator. Feedwater enters the steam generator through the feedwater sparger and flows into the downcomer where it mixes with the recirculation saturated water that is being returned from the moisture separators. The combined flow moves through the downcomer and enters the tube bundle region at the bottom of the steam generator. As fluid rises through the tube bundle region, it absorbs heat from the U-tube in which the primary coolant flows. This causes steam formation. The resulting two-phase mixture rises until it reaches the separators which remove liquid from the steam, return the liquid to the downcomer for further recirculation, and allow the steam to rise to the dryers. The recirculation process is sustained by an imbalance in the hydraulic head of the fluid between the downcomer and the tube bundle region. At high power operation, this driving force is significant and recirculation flow is dominant. However, at low power the amount of boiling in the tube bundle region is insufficient to create driving head for lots of recirculation flowrates. Hence, as the power level decreases, the recirculation flowrate also decreases.

Steam generator level 'shrink and swell' refers to

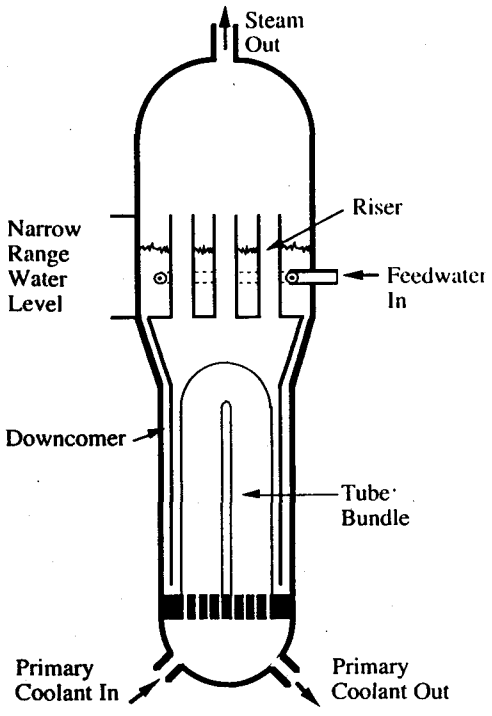

Fig. 1. Schematic of U-tube Steam Generator

temporary changes in the water level in the downcomer region that occur whenever a steam bubble suddenly collapses or forms in the tube bundle region. For example, on collapse of a steam bubble, the volume taken by the two-phase mixture suddenly decreases and is filled with liquid from the downcomer region. Hence, the indicated and measured levels, which are obtained from the downcomer, drop even though the mass of fluid in the steam generator has risen. This phenomenon is referred to as level shrink. Swelling is essentially the reverse effect. Shrink and swell may be caused by either a change in the feedwater or steam flowrates or by a change in feedwater temperature. However, the mechanisms involved are different. First, consider the effect of changing the feedwater flowrate. Introduction of feedwater at a temperature below saturation in the tube bundle region will cause internal condensation. Thus, a sudden increase in feedwater flowrate will momentarily reduce the boiling rate and cause outflow from the downcomer. Hence, the downcomer level will initially decrease even though the long-term effect of the increase feedwater flow will be to raise the level because of mass unbalance. Next consider the effect of changing the steam flowrate. A decreased in steam flowrate will cause steam generator pressure to rise which will collapse the existing steam bubble in the tube bundle region. Higher pressure will also cause an increase in the saturation temperature which in turn will reduce heat transfer from the primary coolant. Therefore, the boiling rate will decrease following a steam flowrate decrease. The long-term effect will be a level increase because the rate of mass removal from the steam generator is reduced. However, the immediate impact will be decrease of level as water flows out of the downcomer and into the volume formerly occupied by the collapsed steam bubbles. Another initiator of shrink and swell effects is the primary coolant temperature. For example, a primary coolant temperature decrease that results from a reactor power drop will cause a decrease in both the heat transfer rate from the primary coolant and the boiling rate in the tube bundle region that occurs before the boiling rate changes. Hence, once again the immediate effect is outflow from the downcomer even though the long-term trend will be for downcomer level to rise.

Figure 2 is from a simulation study that shows the effect of a step increase in feedwater flowrate(5kg/s) on the observed steam generator water level. Curves are given for several different power levels. In each case, the level first rises, then drops (shrink effect), and then again rises as asymptotic conditions that reflect the increase in feedwater flowrate are achieved. The initial small rise in level is the result of the mass increase in the downcomer region that occurs before the boiling rate changes. However, the increase in downcomer hydraulic head soon causes an increase of flow into the tube bundle region and this causes the level to shrink.

Shrink and swell are an example of an 'inverse response' in that the initial change in the controlled parameter is in the opposite direction to its asymptotic behavior. Such responses are exhibited by certain other processing units including drum boilers (level) and distillation columns (temperature) [2, 3]. Ilinoya and Altpeter investigated this phenomenon and found that the transfer functions for systems that exhibit inverse responses contain a zero in the right half-plane of the Laplace domain [4]. For example, consider the following transfer which combines an in-

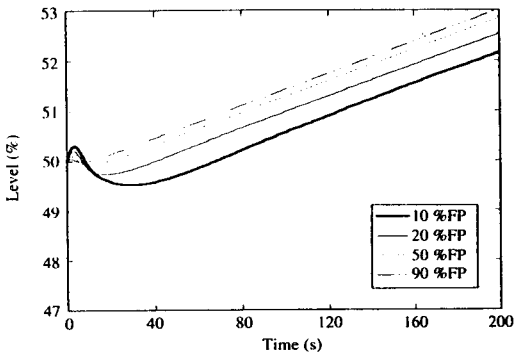

Fig. 2. Steam Generator Level Shrink Effect as Results of a Step Increase in Feedwater Flow

tegral term and a negative first order lag:

$$\frac{\bar{y}(s)}{\bar{f}(s)} = \frac{K_2}{s} - \frac{K_1}{\tau s + 1} \quad (1)$$

This system has poles at 0 and $-1/\tau$ and a zero at $K_2/(K_1 - K_2\tau)$. If $K_2\tau$ is less than K_1 then the system has a positive zero and its response to a step change in input is inverse in nature. This occurs because the first order term dominates initially and the overall response is therefore temporarily opposite to its asymptotic one. However, if the condition $K_2\tau$ is less than K_1 is not satisfied, an inverse response does not occur.

3. Steam Generator Simplified Model

Previous work had resulted in the development and validation against actual plant data of a detailed, non-linear model of steam generator dynamics [5]. This model's complexity made it impractical for use as the basis of a controller. In order to overcome this difficulties, the steam generator simplified model was used. Irving and Bihoreaux have suggested a transfer function that successfully describes the shrink and swell effects that are created by feedwater or steam flowrate changes [6]. The inputs to the equation are feedwater and steam flowrates. The output is the downcomer water level. The equation is:

$$L_w(s) = \left[\frac{G_1}{s} - \frac{G_{2f}}{\tau_{2f}s+1} + \frac{G_{3f}}{(s+1/\tau_{3f})^2+\omega^2}\right]\dot{m}_{fw}(s) + \left[-\frac{G_1}{s} + \frac{G_{2s}}{\tau_{2s}s+1}\right]\dot{m}_s(s) \quad (2)$$

where $L_w(s)$ is the Laplace transform of the steam generator level change due to feedwater or steam flowrate changes, $\dot{m}_{fw}(s)$ and $\dot{m}_s(s)$ are the Laplace transforms of the changes in feedwater and steam flowrate respectively. Each term of Equation (2) has physical significance. G_1/s is the mass capacity term of the steam generator where G_1 is a measure of the steam generator's height to volume ratio. This mass capacity term represents changes in the steam generator level caused by mass influx or efflux from the volume of the particular steam generator. If the G_1/s term were the only quantity in the level equation, then the downcomer level indicator would be an accurate representation of the mass contained in the steam generator. The $G_{2f}/(\tau_{2f}s+1)$ and $G_{2s}/(\tau_{2s}s+1)$ terms are the first order and represent the shrink and swell effects. G_{2f} and G_{2s} are variables that describe the magnitude of the shrink and swell effects that result from changes in feedwater and steam flowrate respectively. These two values depend on the operating power of the reactor. The quantities τ_{2f} and τ_{2s} are the characteristic decay times for the shrink and swell effects caused by the feedwater and steam flowrate changes, respectively. The remaining term in Equation (2) describes the mechanical oscillation that results from the direct addition of feedwater to the steam generator. This quantity appears only in response to a feedwater change and it decays rapidly.

However, Equation (2) does not include the effect of a change in primary coolant temperature which, as noted earlier, can cause shrink or swell effects. These effects are represented by the addition of two opposing first order terms:

$$L_T(s) = \left[\frac{G_{1T}}{(1+\tau_{1T}s)} - \frac{G_{2T}}{(1+\tau_{2T}s)}\right]T_p(s) \quad (3)$$

where $L_T(s)$ is the Laplace transform of the steam generator level change that results from a primary coolant temperature change and $T_p(s)$ is the Laplace transform of the change in primary coolant temperature. G_{1T} and G_{2T} are variables that describe the magnitude of the shrink and swell effects that result from changes in feedwater and steam flowrate respectively. These two values depend on the operating power of the reactor. The quantities and τ_{2f} and τ_{2s} are the characteristic decay times for the shrink and swell effects-caused by the feedwater and steam flowrate changes, respectively.

The steam generator level response is therefore the sum of the individual responses to the three different inputs and is as follows:

$$L(s) = G_{fw}(s)\dot{m}_{fw}(s) + G_s(s)\dot{m}_s(s) + G_T(s)T_p(s) \quad (4)$$

where,

$$G_{fw}(s) = \frac{L_{fw}(s)}{\dot{m}_{fw}(s)} = \frac{G_1}{s} - \frac{G_{2f}}{(\tau_{2f}s+1)} + \frac{G_{3f}s}{(s+1/\tau_{3f})^2+\omega^2} \quad (5)$$

$$G_s(s) = \frac{L_s(s)}{\dot{m}_s(s)} = -\frac{G_1}{s} + \frac{G_{2s}}{(\tau_{2s}s+1)} \quad (6)$$

$$G_T(s) = \frac{L_T(s)}{T_p(s)} = \frac{G_{1T}}{(1+\tau_{1T}s)} - \frac{G_{2T}}{(1+\tau_{2T}s)} \quad (7)$$

and where $L_{fw}(s)$, $L_s(s)$ and $L_T(s)$ are the Laplace transforms of the steam generator level change that result from perturbations in feedwater flowrate, steam flowrate and primary coolant temperature respectively. The quantities $G_{fw}(s)$, G_s and $G_T(s)$ are the process transfer functions of the feedwater flowrate, steam flowrate and primary coolant temperature change respectively.

The next step in the modeling process was parameter identification. Equations (4-7) were converted to the time domain and the appropriate value for each coefficient was then found by minimizing the quadratic error between the response to step perturbations of the simplified and detailed non-linear models. This was done at different power levels and each coefficient was ultimately described as a polynomial function of power. The model was then validated by comparing the response of the simplified model both to that of the non-linear one and to actual plant data. The detailed results are described in the reference [7]. The resulting agreement was excellent.

4. Controller Design

Figure 3 depicts a current-generation steam generator level controller. The unit is a three-element PI design that combines feedback based on a level error with feedforward action based on a flowrate error. For the former, the error is generated by comparing the level setpoints and the measured level. For the

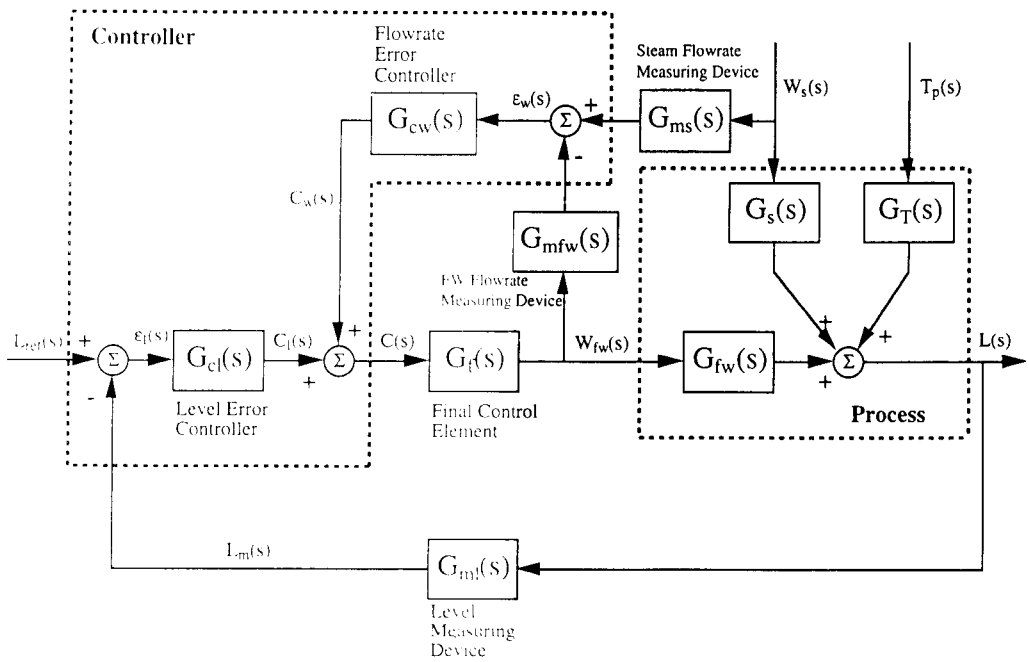

Fig. 3. Block Diagram of Current Generation Steam Generator Water Level Controller

latter, the error is computed as the difference between steam and feedwater flowrates. The overall control law is :

$$\dot{m}_{fw}(s) = K_l\left(1+\frac{1}{T_l s}\right)\varepsilon_l + K_w\left(1+\frac{1}{T_w s}\right)\varepsilon_w \qquad (8)$$

where K_l is the proportional level gain, T_l is the level error integration time, ε_l is the level error($L_{ref}-L$), K_w is the proportional flowrate gain, T_w is the flowrate error integral time, ε_w is the flowrate error($\dot{m}_s-\dot{m}_{fw}$), and L_{ref} is the reference steam generator water level. A major problem associated with this controller is that the flowrate measurements become so uncertain at low power levels as to be unusable. Shrink and swell effects therefore become exacerbated with the result that level control may be lost. Should this occur, a plant trip would be necessary. Accordingly, the objective here was to design a controller that would give excellent performance at all power levels. The approach taken was to develop model-based compensators that cancel the effect of the inverse response behavior on the steam generator water level measurements. For this purpose, the simplified transfer function was used as the model and compensators were designed for feedwater and steam flowrate and for primary temperature. That for feedwater flowrate will be described in some detail below.

Figure 4 is a block diagram of the feedwater flowrate compensator. The feedwater flowrate is controlled to maintain the desired steam generator level by the level PI controller. In this paper, the control element and level measuring device models are not included and assumed to be work perfectly. As shown in this figure, the measured level signal is modified by a compensation signal which is generated by the feedwater compensator based on the feedwater change signal. Finally input signal to the PI controller becomes :

$$L^*(s) = L_m(s) + L_c(s) \qquad (9)$$

where $L^*(s)$ is the Laplace transform of the compensated level signal that will be used as input to the PI

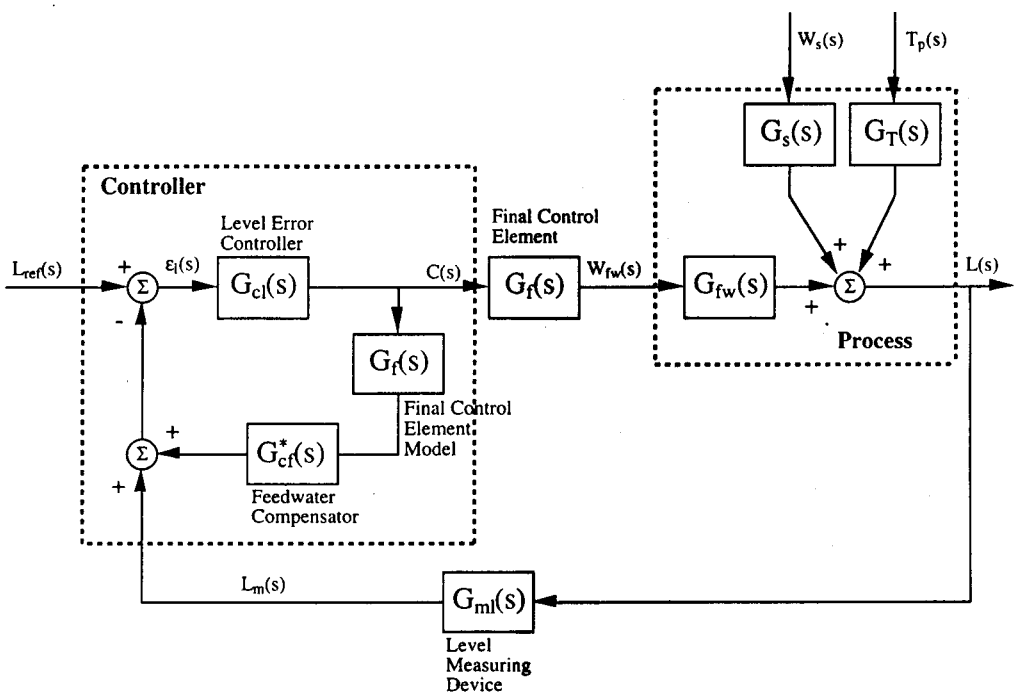

Fig. 4. Block Diagram of Feedwater Flowrate Compensator

controller, $L_m(s)$ is the Laplace transform of the measured level signal, and $L_c(s)$ is the Laplace transform of the compensation signal. For it to be effective, the compensation signal should contain both an inverse response and mass oscillation term. The compensator is therefore most readily designed by using the transfer functions for those two terms except with opposite sign. Thus,

- For the inverse response : $\dfrac{G_{2f}}{\tau_{2f}s+1}$ (10)

- For the mass oscillation : $-\dfrac{G_{3f}s}{\left(s+1/\tau_{3f}\right)^2+\omega^2}$ (11)

The compensation signal should decay to zero under steady state conditions. Otherwise, the controlled level will exhibit a steady-state offset. The mass oscillation term does die out at steady-state. However, because the inverse response transfer function consists of a first-order lag term, the compensation signal as a whole does not do likewise. To overcome this difficulty, Surgenor suggested a compensator that consists of an inverse response predictor and an impulse function [7]. The compensator for feedwater flowrate then has the following form :

$$G^*_{cf} = \frac{G_{2f}}{\tau_{2f}s+1}\cdot\frac{\alpha_f s}{\alpha_f s+1} - \frac{G_{3f}s}{\left(s+1/\tau_{3f}\right)^2+\omega^2} \quad (12)$$

where G^*_{cf} is the transfer function of the feedwater compensator and α_f is an adaptive parameter that determines the amount of compensation. If α_f is set to zero, no compensating action for the inverse response is taken and the controller is the same as a conventional one. If α_f is set to infinity, the inverse response is completely compensated. However, the difficulty associated with the compensation signal in not going to zero at steady-state then returns.

The compensation signal is then found by taking the product of the feedwater compensator and the feedwater flowrate :

$$L_c(s) = G^*_{cf}\, m_f(s) \quad (13)$$

Simulation studies were conducted to determine the time behavior of the compensated level after a step increase in feedwater flowrate at 10% full power. It was found that as α_f increases, the inverse response is diminished but the steady-state offset error increases. The effect of α_f on compensator stability was also examined by replacing the loop shown in Figure 4 with an equivalent single loop. The resulting series compensator was then applied to the process to obtain the transfer function for the closed-loop system. Root locus analyses showed this system to be unconditionally stable for values of α_f in excess of 100s. For values of α_f less than 100s stability depended on the feedback gain.

Load parameters, such as steam flowrate and primary coolant temperature, also result in an inverse response. This is especially true for steam generators where the level setpoint remains constant while the load changes. Accordingly, compensators were also designed for the steam flowrate and primary coolant temperature. For steam flowrate, the compensator is :

$$G^*_{cs} = -\frac{G_{2s}}{\tau_{2s}s+1}\cdot\frac{\alpha_s s}{\alpha_s s+1} \quad (14)$$

where G^*_{cs} is the transfer function of the steam flowrate compensator and α_s is the adaptive parameter that determines the amount of compensation and precludes an offset error at steady-state. For the primary coolant temperature, the compensator is :

$$G^*_{cT}(s) = -G_{1T}\left(\frac{1}{1+\tau_{1T}s} - \frac{1}{1+\tau_{2T}s}\right) \quad (15)$$

where advantage has been taken of the near equality of G_{1T} and G_{2T}. This expression decays to zero at steady-state. Hence, no impulse function is needed.

Finally, feedforward control action is added to improve performance. This entailed adding the change in the estimated steam flowrate directly to the PI controller's output. It was also observed that steam generator mass inventory decreases as power increases because more vapor exists at higher power. Therefore, the mass inventory should be offset when pow-

er increases and supplemented when power decreases. Dynamic lag compensation was used for this purpose. Thus,

$$\dot{m}_{ff}(s) = \frac{1}{\alpha_{ff} s + 1} \dot{m}_{se}(s) \quad (16)$$

where $\dot{m}_{ff}(s)$ is the Laplace transform of the feedforward controller output, $\dot{m}_{se}(s)$ is that of the estimated steam flowrate, and α_{ff} is the time constant for the lagged response.

Figure 5 is a schematic of the final control system. It consists of a PI controller and three different compensators designed to offset the inverse response associated with feedwater flowrate, steam flowrate and primary coolant temperature.

5. Controller Evaluation

Simulation studies were conducted in which the proposed controller was evaluated by application to several different transients. The aforementioned detailed non-linear model was used to simulate level response. Figure 6 shows the steam generator level following a step perturbation in the feedwater flowrate. The reactor was at 10% of rated power. Hence, the use of flow measurements to anticipate level changes was not possible. Shown in the figure are the response of both an existing analog level controller and that of the one designed here using compensators. The former was tuned via the Ziegler-Nichols method to avoid divergence. [8] The latter is shown for three sets of feedback gains and error integral times. All

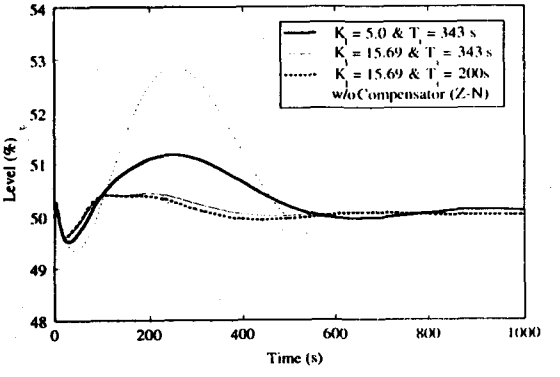

Fig. 6. Steam Generator Level During Feedwater Flowrate Perturbation Transient at 10%FP

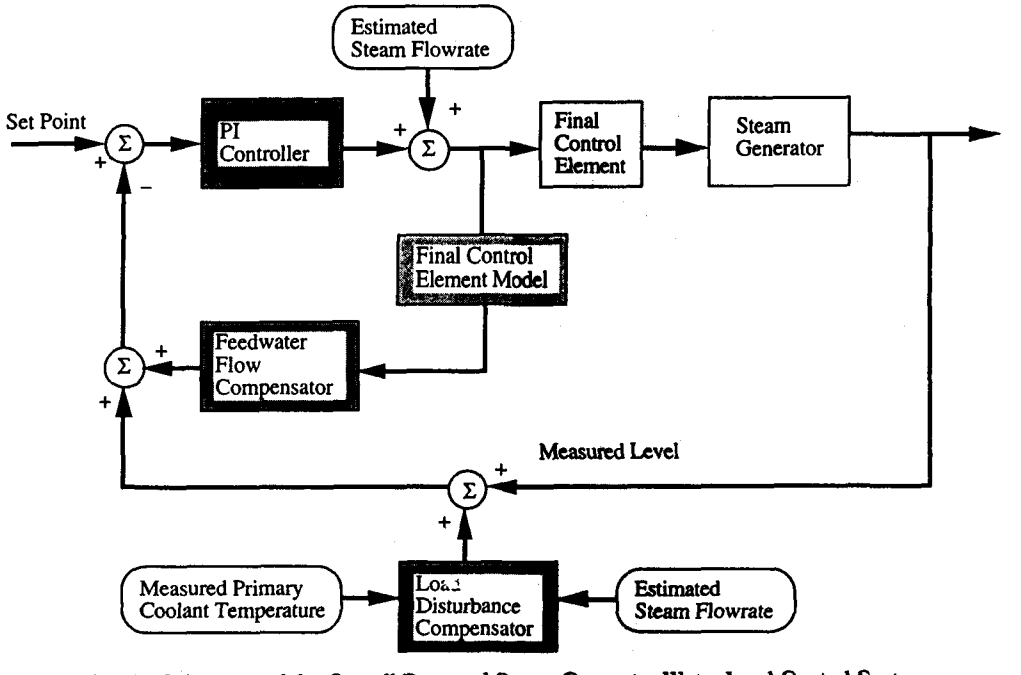

Fig. 5. Schematic of the Overall Proposed Steam Generator Water Level Control System

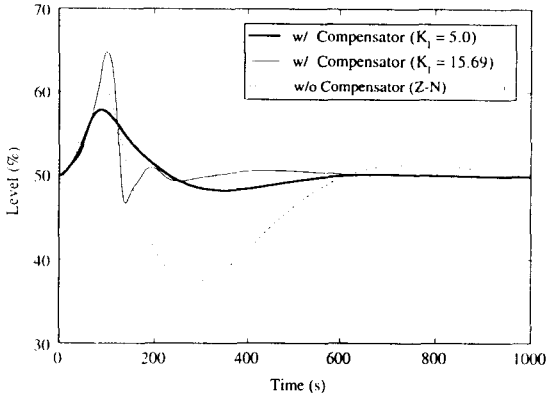

Fig. 7. Steam Generator Level During Power Ramp from 10%FP to 15%FP at a 5.0%/Minute Ramp Rate

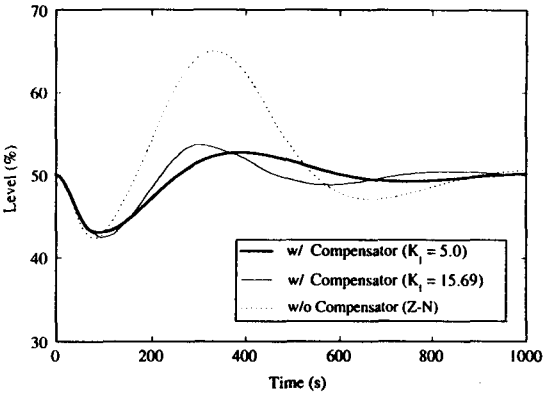

Fig. 8. Steam Generator Level During Power Ramp from 15%FP to 10%FP at a 5.0%/Minute Ramp Rate

four cases showed stable level trends. However, the compensated controller's performance was superior.

Figure 7 shows the steam generator level both during and following a power ramp from 10% to 15% of full power at a ramp rate of 5% per minute. Figure 8 gives the same information for a ramp from 15% to 10% full power. Shown are the response of both an existing analog and the compensated controller. The former was again tuned via the Ziegler-Nichols method while the latters behavior is shown for two different gains. In each case, stable level trends resulted. However, the compensated controller significantly improved performance. Both additional simulation studies and a further discussion of the controller's design are available [9].

The proposed controller adopts inverse response compensation techniques which are derived from a simplified transfer function model. In other to show the proposed controllers robustness to the parameters of compensator, a simple sensitivity analysis was performed. It was assumed that the compensator was designed based on the incorrect parameters. An error of 50% was either added or subtracted to all correct parameters. Figure 9 shows the steam generator level both during and following a power ramp from 10% to 15% of full power at a ramp rate of 5% per minute. As shown in this figure, inaccurately compensated controller also stabilized level disturbance with its performance being slightly degraded.

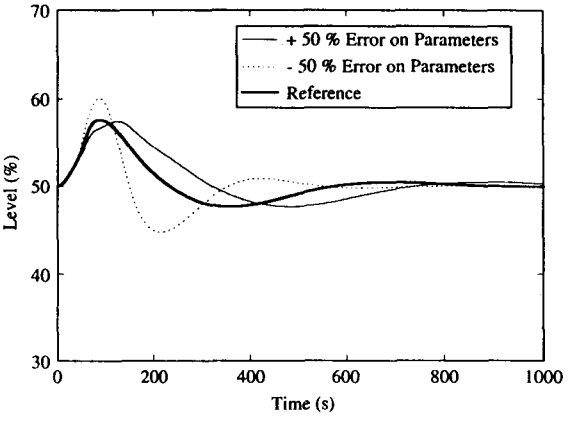

Fig. 9. Steam Generator Level During Power Ramp from 10%FP to 15%FP at a 5.0%FP/Minute Ramp Rate When the Compensators are Designed with Incorrect Parameters

6. Conclusion

Improved steam generator level control performance can be obtained through the use of a model-based compensation technique. Compensators for feedwater flowrate, steam flowrate, and primary coolant temperature were developed from a simpli-

fied transfer function model for the purpose of offsetting inverse response behavior. This compensator-based controller can be used over whole power range and ensures stability at both low and high power. Simulation studies of various transients showed that the use of this new controller could greatly reduce the effect of inverse response and significantly improve the controllability of steam generator level.

References

1. G. Singh et al. "Design and Operation of a Digital Low-Power Feedwater Control System for PWRs," EPRI-NP-6149, January (1989)
2. F.G. Shinskey, Process Control Systems : Application, Design, and Tuning, Mcgraw-Hill, New York, (1989)
3. F.H. Yocum, and J.M. Zimmerman, "Real Time Control of Inverse Response Using Dynamic Matrix Control," Proceedings of the American Control Conference, Vol. 88, pp. 266-269 (1989)
4. K. Ilinoya, and R.J. Altpeter, "Inverse Response in Process Control," Industrial and Engineering Chemistry, Vol. 54, No. 7, pp. 39-43, July (1962)
5. J.I. Choi, "Non-Linear Digital Computer Control for the steam Generator System in a Pressurized Water Reactor Plant," Ph. D. Thesis, Department of Nuclear Engineering. Massachusetts Institute of Technology, Cambridge, MA, August (1987)
6. E. Irving, and C. Bihoreaux, "Adaptive Control of No-Minimum Phase Systems Application to the PWR Steam Generator Water Level Control," Proceedings of the 19th IEEE Control and Decision Conference, Albuquerque, NM, pp. 274-279, (1980)
7. B.W. Surgenor, and G. Jie, "Evaluation of a Digitally Compensated Drum Water Level Controller," Instrumentation in the Power Industry, Vol. 30, pp. 85-92, (1987)
8. G. Stephanopoulos, Process Control : An Introduction to Theory and Practice , Prentice-Hall, Inc. NJ, (1984)
9. K.K. Kim, "Design and Simulation of a Digital Control System for a Multi-Modular Power Plant," Ph. D. Thesis, Department of Nuclear Engineering, Massachusetts Institute of Technology, Cambridge, MA, August (1992)